



Ideas and perspectives: hydrothermally driven redistribution and sequestration of early Archaean biomass – the “hydrothermal pump hypothesis”

Jan-Peter Duda^{1,2}, Volker Thiel¹, Thorsten Bauersachs³, Helge Mißbach^{1,4}, Manuel Reinhardt^{1,4}, Nadine Schäfer^{1,2}, Martin J. Van Kranendonk^{5,6,7}, and Joachim Reitner^{1,2}

¹Department of Geobiology, Geoscience Centre, Georg-August-Universität Göttingen, Goldschmidtstraße 3, 37077 Göttingen, Germany

²“Origin of Life” Group, Göttingen Academy of Sciences and Humanities, Theaterstraße 7, 37073 Göttingen, Germany

³Department of Organic Geochemistry, Institute of Geosciences, Christian-Albrechts-Universität Kiel, Ludewig-Meyn-Straße 10, 24118 Kiel, Germany

⁴Department Planets and Comets, Max Planck Institute for Solar System Research, Justus-von-Liebig-Weg 3, 37077 Göttingen, Germany

⁵Australian Centre for Astrobiology, University of New South Wales, Kensington, New South Wales 2052, Australia

⁶School of Biological, Earth and Environmental Sciences, University of New South Wales, Kensington, New South Wales 2052, Australia

⁷Australian Research Council Centre of Excellence for Core to Crust Fluid Systems, School of Biological, Earth and Environmental Sciences, University of New South Wales, Kensington, New South Wales 2052, Australia

Correspondence: Jan-Peter Duda (jan-peter.duda@geo.uni-goettingen.de)

Received: 1 December 2017 – Discussion started: 5 December 2017

Revised: 6 February 2018 – Accepted: 8 February 2018 – Published: 15 March 2018

Abstract. Archaean hydrothermal chert veins commonly contain abundant organic carbon of uncertain origin (abiotic vs. biotic). In this study, we analysed kerogen contained in a hydrothermal chert vein from the ca. 3.5 Ga Dresser Formation (Pilbara Craton, Western Australia). Catalytic hydrolysis (HyPy) of this kerogen yielded *n*-alkanes up to *n*-C₂₂, with a sharp decrease in abundance beyond *n*-C₁₈. This distribution ($\leq n$ -C₁₈) is very similar to that observed in HyPy products of recent bacterial biomass, which was used as reference material, whereas it differs markedly from the unimodal distribution of abiotic compounds experimentally formed via Fischer–Tropsch-type synthesis. We therefore propose that the organic matter in the Archaean chert veins has a primarily microbial origin. The microbially derived organic matter accumulated in anoxic aquatic (surface and/or subsurface) environments and was then assimilated, redistributed and sequestered by the hydrothermal fluids (“hydrothermal pump hypothesis”).

1 Introduction

Extensive hydrothermal chert vein systems containing abundant organic carbon are a unique phenomenon of early Archaean successions worldwide (Lindsay et al., 2005; Van Kranendonk, 2006; Hofmann, 2011). A dense stockwork of several hundred kerogen-rich hydrothermal chert veins that penetrate footwall pillowed komatiitic basalts of the ca. 3.5 Ga Dresser Formation (Pilbara Craton, Western Australia; Fig. 1) are up to 2 km deep by 25 m wide (Hickman, 1973, 1983; Nijman et al., 1999; Van Kranendonk and Pirajno, 2004; Lindsay et al., 2005; Van Kranendonk, 2006; Van Kranendonk et al., 2008) (Fig. S1 in the Supplement). Depleted stable carbon isotope signatures ($\delta^{13}\text{C}$) of bulk kerogens (−38.1 to −24.3‰) and of organic microstructures (−33.6 to −25.7‰) in these hydrothermal chert veins, as well as remnants of what appear to be microbial remains, are consistent with a biological origin of the organic matter (Ueno et al., 2001, 2004; Glikson et al., 2008; Pinti et al., 2009; Morag et al., 2016). Problematically, however, simi-

larly depleted $\delta^{13}\text{C}$ values (partly down to ca. -36‰ relative to the initial substrate) can also be formed through abiotic processes, for instance via Fischer–Tropsch-type synthesis (McCollom et al., 1999; McCollom and Seewald, 2006), and putative microbial remains are not always reliable (Schopf, 1993; Brasier et al., 2002, 2005; Schopf et al., 2002; Bower et al., 2016).

Organic biomarkers can help to trace life and biological processes through deep time and add important information on the origin of the organic matter, even in very old sedimentary rocks (Brocks and Summons, 2003; Summons and Hallmann, 2014). In Archaean rocks, however, molecular fingerprints in the conventionally analysed bitumen (i.e. the extractable portion of organic matter) are commonly blurred by thermal maturation and/or ancient or modern contamination (Brocks et al., 2008; Gérard et al., 2009; Brocks, 2011; French et al., 2015). In contrast, the non-extractable portion of organic matter, known as kerogen, tends to be less affected by thermal maturation and contamination and is considered to be syngenetic with the host rock (Love et al., 1995; Brocks et al., 2003b; Marshall et al., 2007; Lockhart et al., 2008). Catalytic hydrolysis (HyPy) is a powerful tool for sensitively releasing kerogen-bound hydrocarbon moieties with little structural alteration (Love et al., 1995). HyPy has been successfully applied to Archaean kerogens in rocks from the Pilbara Craton, liberating syngenetic organic compounds consistent with a biogenic origin (Brocks et al., 2003b; Marshall et al., 2007). However, this technique has not yet been used on kerogens contained in hydrothermal chert veins of this age.

Here, we present the results of analyses of kerogen embedded in a freshly exposed hydrothermal chert vein of the ca. 3.5 Ga Dresser Formation. Our analyses include field and petrographic observations, Raman spectroscopy and organic geochemistry ($\delta^{13}\text{C}_{\text{TOC}}$; kerogen-bound molecules via HyPy followed by gas chromatography – mass spectrometry (GC-MS) and gas chromatography – combustion – isotope ratio mass spectrometry (GC-C-IRMS)). To further constrain potential sources of the Dresser kerogen, we additionally applied HyPy on (i) excessively pre-extracted cyanobacterial biomass and (ii) produced abiotic organic matter via Fischer–Tropsch-type synthesis using a hydrothermal reactor. Results of these investigations suggest that the Dresser kerogen has a primarily microbial origin. We hypothesize that biomass-derived organic compounds accumulated in anoxic aquatic environments and were then redistributed and sequestered by subsurface hydrothermal fluids (“hydrothermal pump hypothesis”).

2 Material and methods

2.1 Sample preparation

A fresh decimetre-sized sample of a Dresser chert vein was obtained from a recent cut wall of the abandoned Dresser Mine in the Pilbara Craton, Western Australia (GPS: $21^{\circ}09'04.13''\text{S}$; $119^{\circ}26'15.21''\text{E}$; Figs. 1, S1d; for geological maps, see Hickman, 1983; Van Kranendonk, 1999; Hickman and Van Kranendonk, 2012). The external surfaces (ca. 1–2 cm) of the sample block were removed using an acetone-cleaned rock saw and then used for the preparation of thin sections. The surfaces of the resulting inner block were extensively rinsed with acetone and then removed (ca. 1–2 cm) with an acetone-cleaned high precision saw (Buehler; Isomet 1000, Germany). The surfaces of the resulting sample were again rinsed with acetone and then crushed and powdered using a carefully acetone-cleaned pebble mill (Retsch MM 301, Germany).

2.2 Petrography and Raman spectroscopy

Petrographic analysis was conducted using a Zeiss SteREO Discovery.V8 stereomicroscope (transmitted and reflected light) linked to an AxioCam MRC5 5-megapixel camera.

Raman spectra were recorded using a Horiba Jobin Yvon LabRam-HR 800 UV spectrometer (focal length of 800 mm) attached to an Olympus BX41 microscope. For excitation an Argon ion laser (Melles Griot IMA 106020B0S) with a laser strength of 20 mW was used. The laser beam was focused onto the sample using an Olympus MPlane 100 \times objective with a numerical aperture of 0.9 and dispersed by a 600 Lmm^{-1} grating on a charge-couple device (CCD) detector with 1024×256 pixels. This yielded a spectral resolution of $< 2 \text{ cm}^{-1}$ per pixel. Data were acquired over 10 to 30 s for a spectral range of 100–4000 cm^{-1} . The spectrometer was calibrated by using a silicon standard with a major peak at 520.4 cm^{-1} . All spectra were recorded and processed using the LabSpec™ database (version 5.19.17; Jobin Yvon, Villeneuve d'Ascq, France).

2.3 Raman-derived H / C data

H/C values were calculated based on integrated peak intensities of Raman spectra using the formula $\text{H/C} = 0.871 \cdot I_{\text{D5}} / (I_{\text{G+D2}}) - 0.0508$ (Ferralis et al., 2016). The peaks were fitted in the LabSpec™ software (see Sect. 2.2) using the Gauss/Lorentz function.

2.4 Molecular analysis of the Dresser kerogen

All materials used for preparation were heated to 500 °C for 3 h and/or extensively rinsed with acetone prior to sample contact. A laboratory blank was prepared and analysed in parallel to monitor laboratory contaminations.

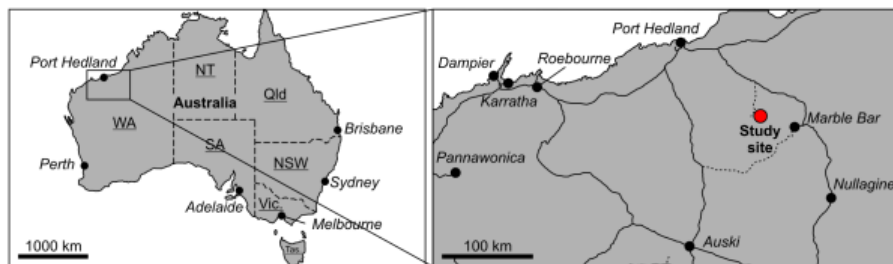


Figure 1. Location of the study site in Western Australia. The hydrothermal chert vein analysed occurs in a recent cut wall of the abandoned Dresser Mine close to Marble Bar.

We applied catalytic hydropyrolysis (HyPy) to release molecules from the Dresser kerogen and pre-extracted biomass of the heterocystous cyanobacterium *Anabaena cylindrica* SAG 1403-2 following previously published protocols (Snape et al., 1989; Love et al., 1995, 2005). HyPy allows the breaking of covalent bonds by progressive heating under high hydrogen pressure (150 bar). The released products are immediately removed from the hot zone by a constant hydrogen flow and trapped downstream on clean, combusted silica powder cooled with dry ice (Meredith et al., 2004). All hydropyrolysates were eluted from the silica trap with high-purity dichloromethane (DCM), desulfurized overnight using activated copper and subjected to gas chromatography – mass spectrometry (GC-MS). Before all experiments, the empty HyPy system was heated (ambient temperature to 520 °C, held for 30 min) to remove any residual molecules.

Isolation of the Dresser kerogen followed standard procedures (cf. Brocks et al., 2003b). 57 g of powdered sample was first demineralized with hydrochloric acid (24 h) and then hydrofluoric acid (11 days). The purified organic matter was then exhaustively extracted using three excess volumes of DCM and *n*-hexane, respectively ($\times 3$), ultrasonic swelling in pyridine (2×20 min at 80 °C), and ultrasonic extraction with methanol, DCM ($\times 3$) and DCM / methanol (1/1; *v/v*). The kerogen was subsequently extracted with *n*-hexane until no more compounds were detected via GC-MS. The pure kerogen was used for HyPy following an experimental protocol optimized for the analysis of Archaean kerogens (Brocks et al., 2003b; Marshall et al., 2007).

In order to monitor potential contamination, we applied HyPy to blanks before and after the kerogen run. The Dresser kerogen (131.06 mg) and blanks were sequentially heated in the presence of a sulfided molybdenum catalyst (10 wt %) and under a constant hydrogen flow ($5 \text{ dm}^3 \text{ min}^{-1}$) using a two-step approach (cf. Brocks et al., 2003b; Marshall et al., 2007; Fig. S2). The low-temperature step included heating from ambient temperature to 250 °C ($300 \text{ }^\circ\text{C min}^{-1}$) and then to 330 °C ($8 \text{ }^\circ\text{C min}^{-1}$) to release any molecules that were strongly adsorbed to the kerogen and not accessible to solvent extraction. The silica powder was subsequently recovered from the product trap, and the trap was refilled

with clean, combusted silica powder for the following high-temperature step. This step included heating from ambient temperature to 520 °C ($8 \text{ }^\circ\text{C min}^{-1}$) to release molecules covalently bound to the kerogen.

2.5 Molecular analysis of pre-extracted cyanobacterial biomass (*Anabaena cylindrica*)

We used cell material of the heterocystous cyanobacterium *Anabaena cylindrica* strain SAG 1403-2 as it fulfils all criteria for reference material (availability, well characterized, etc.). The material was obtained from the Culture Collection of Algae at the Georg-August-Universität Göttingen (Germany) and grown at the Christian-Albrechts-Universität Kiel (Germany). The axenic batch culture was maintained in 250 mL of BG11₀ medium free of combined nitrogen sources (Rippka et al., 1979) at 29 °C. A light : dark regime of 14 h : 10 h with a photon flux density of $135 \mu\text{mol photons m}^{-2} \text{ s}^{-1}$ was provided by a white fluorescent light bulb. At the end of the logarithmic growth phase, cells were harvested by centrifugation, and they were lyophilized thereafter. Subsequently, an aliquot of the freeze-dried biomass was exhaustively extracted following the methodology described by Bauersachs et al. (2014).

HyPy was performed following an experimental protocol optimized for biomass applications (Love et al., 2005). Briefly, the material was heated in the presence of a sulfided molybdenum catalyst (1.5 times the weight of the bacterial extraction residue) and under a constant hydrogen flow ($6 \text{ dm}^3 \text{ min}^{-1}$). The HyPy program included heating from ambient temperature to 260 °C ($300 \text{ }^\circ\text{C min}^{-1}$) and then to 500 °C ($8 \text{ }^\circ\text{C min}^{-1}$).

2.6 Fischer–Tropsch-type synthesis of organic matter under hydrothermal conditions

Fischer–Tropsch-type reactions were carried out based on McCollom et al. (1999). A mixture of 2.5 g oxalic acid (dihydrate, suprapur[®], Merck KGaA), 1 g montmorillonite (K10, Sigma Aldrich; pre-extracted with DCM; $\times 4$) and ca. 11 mL ultrapure water was heated to 175 °C for 66 to 74 h in a sealed Morey-type stainless steel autoclave. The autoclave

was rapidly (≤ 15 min) cooled to room temperature with compressed air.

Fluid and solid phases were collected and extracted with DCM ($\times 4$). The montmorillonite was removed by centrifugation and filtration with silica powder and sea sand (which were combusted prior to use). The obtained extracts were then concentrated by rotary evaporation (40 °C, 670 mbar) and subjected to GC-MS analysis. Analytical blank experiments were carried out with all reactants to keep track of contamination.

2.7 Gas chromatography – mass spectrometry

GC-MS analysis of HyPy products was carried out with a Thermo Scientific Trace 1310 GC coupled to a Thermo Scientific Quantum XLS Ultra MS. The GC instrument was equipped with a capillary column (Phenomenex Zebron ZB-5, 30 m, 0.25 μm film thickness, 0.25 mm inner diameter). Fractions were injected into a splitless injector and transferred to the GC column at 270 °C. He was used as carrier gas with a constant flow rate of 1.5 mL min⁻¹. The GC oven temperature was held isothermal at 80 °C for 1 min and then ramped to 310 °C at 5 °C min⁻¹, at which it was kept for 20 min. Electron ionization mass spectra were recorded in full-scan mode at an electron energy of 70 eV with a mass range of m/z 50–600 and scan time of 0.42 s.

2.8 Polyaromatic hydrocarbon ratios

Polyaromatic hydrocarbons (PAHs) are organic compounds consisting of multiple fused benzene rings. Methylation and isomerization characteristics of various GC-amenable PAHs are altered during maturation and thus provide a measure for assessing the thermal maturity of organic matter (Killops and Killops, 2005; Peters et al., 2005). The following PAH maturity parameters were used in this study:

1. methylnaphthalene ratio (MNR) = 2-MN / 1-MN (Radke et al., 1984),
2. methylphenanthrene index (MPI-I) = $1.5 \cdot (2\text{-MP} + 3\text{-MP}) / (P + 1\text{-MP} + 9\text{-MP})$ (Radke and Welte, 1983), and
3. computed vitrinite reflectance [R_c (MPI-I)] = $0.7 \cdot \text{MPI-I} + 0.22$ (according to $P/\text{MP} > 1$; Boreham et al., 1988).

MN stands for methylnaphthalene, P for phenanthrene and MP for methylphenanthrene.

2.9 Total organic carbon (TOC) and $\delta^{13}\text{C}$ analyses (TOC and compound specific)

TOC, $\delta^{13}\text{C}_{\text{TOC}}$ and compound-specific $\delta^{13}\text{C}$ analyses were conducted at the Centre for Stable Isotope Research and Analysis (KOSI) at the Georg-August-Universität Göttingen,

Germany. Stable carbon isotope data are expressed as delta values relative to the Vienna Pee Dee Belemnite (VPDB) reference standard.

The TOC content and $\delta^{13}\text{C}_{\text{TOC}}$ values were determined in duplicate using an elemental analyser (NA-2500 CE-Instruments) coupled to an isotope ratio mass spectrometer (Finnigan MAT Delta plus). Ca. 100 mg of powdered and homogenized whole rock material were analysed in each run. For internal calibration an acetanilide standard was used ($\delta^{13}\text{C} = -29.6\text{‰}$; SD = 0.1 ‰). TOC content measurements showed a mean deviation of 0.1 wt %. The average $\delta^{13}\text{C}_{\text{TOC}}$ value had a standard deviation of 0.3 ‰.

Compound-specific $\delta^{13}\text{C}$ analyses were conducted with a Trace GC coupled to a Delta Plus isotope ratio mass spectrometer (IRMS) via a combustion interface (all Thermo Scientific). The combustion reactor contained CuO, Ni and Pt and was operated at 940 °C. The GC was equipped with two serially coupled capillary columns (Agilent DB-5 and DB-1; each 30 m, 0.25 μm film thickness, 0.25 mm inner diameter). Fractions were injected into a splitless injector and transferred to the GC column at 290 °C. The carrier gas was He at a flow rate of 1.2 mL min⁻¹. The GC oven temperature program was identical to the one used for GC-MS analysis (see above). CO₂ with a known $\delta^{13}\text{C}$ value was used for internal calibration. Instrument precision was checked using laboratory standards. Standard deviations of duplicate measurements were better than 1.7 ‰.

3 Results

The studied hydrothermal chert vein is hosted in komatiitic pillow basalt that has undergone severe hydrothermal acid-sulfate alteration, producing a kaolinite–illite–quartz mineral assemblage (Van Kranendonk and Pirajno, 2004; Van Kranendonk, 2006) (Fig. S1). The sampled vein crops out in a recent cut wall of the abandoned Dresser Mine (Fig. S1) and consists of a dense chert (microquartz) matrix of deep black colour that contains kerogen and local concentrations of fresh (unweathered) pyrite crystals (Fig. 2a, b). There is no field and/or petrographic evidence for fluid-flow events that post-date the initial vein formation (brecciation textures, etc.).

Petrographic analysis and Raman spectroscopy revealed that kerogen (D bands at 1353 cm⁻¹, G bands at 1602 cm⁻¹) is embedded in the chert matrix (SiO₂ band at 464 cm⁻¹) (see Fig. 2c, for a representative Raman spectrum). The organic matter occurs as small clots (< 50 μm) of variable shape. Raman spectra of the organic matter exhibit relatively wide D and G bands (82 and 55 cm⁻¹ width, respectively) (Fig. 2c). The total organic carbon (TOC) content is 0.2 wt %, and the $\delta^{13}\text{C}_{\text{TOC}}$ value is $-32.8 \pm 0.3\text{‰}$ (Table 1). Raman-derived H/C ratios range between 0.03 and 0.14.

HyPy was applied to the isolated Dresser kerogen, as well as to preceding and subsequent analytical blanks (combusted sea sand). Hydropyrolysates of the preceding blank con-

Table 1. Stable carbon isotopic composition ($\delta^{13}\text{C}$) of the total organic carbon (TOC) and *n*-alkanes released from high-temperature HyPy of the Dresser kerogen.

	<i>n</i> -C ₁₂	<i>n</i> -C ₁₃	<i>n</i> -C ₁₄	<i>n</i> -C ₁₅	<i>n</i> -C ₁₆	<i>n</i> -C ₁₇	<i>n</i> -C ₁₈	<i>n</i> -C _{12–18} (mean)	TOC
$\delta^{13}\text{C}$	−30.3	−33.3	−32.7	−31.1	−29.4	−31.2	−31.7	−31.4	−32.8
SD	0.5	1.4	0.2	1.7	0.3	0.8	0.1	1.2	0.3

Table 2. Maturity indices (based on aromatic hydrocarbons) of the Dresser kerogen. MP/P: methylphenanthrene/phenanthrene ratio; MPI-I: methylphenanthrene index ($1.5 \cdot (2\text{-MP} + 3\text{-MP}) / (P + 1\text{-MP} + 9\text{-MP})$; Radke and Welte, 1983); P/MP: phenanthrene/methylphenanthrene ratio; R_c (MPI-I): computed vitrinite reflectance ($0.7 \cdot \text{MPI-I} + 0.22$, according to $P/\text{MP} > 1$; Boreham et al., 1988); MNR: methyl-naphthalene ratio ($2\text{-MN}/1\text{-MN}$; Radke et al., 1984).

MP/P	MPI-I	P/MP	R _c (MPI-I)	MNR
0.33	0.23	3.01	2.87	2.52

tained a series of *n*-alkanes $\leq n\text{-C}_{24}$, with maximum abundances at *n*-C₁₅ (Figs. 3, S2–S4). Sulfur (only after low-temperature HyPy), traces of siloxanes and a phenol (Figs. 3, S2, S4) were also present. The blank runs also contained traces of aromatic hydrocarbons (Fig. S5).

Low-temperature HyPy of the Dresser kerogen produced traces of C_{14–18} *n*-alkanes, with a maximum at *n*-C₁₅ (Fig. S3). However, these compounds were significantly less abundant than those released during high-temperature HyPy (see below). Other compounds observed in the low-temperature step pyrolysate were elemental sulfur, phenols, phthalic acid, siloxanes and traces of aromatic hydrocarbons (Figs. S2, S4–S5).

High-temperature HyPy of the Dresser kerogen yielded *n*-alkanes ranging from *n*-C₁₁ to *n*-C₂₂ with a notable decrease (“step”) in the abundance of homologues above *n*-C₁₈ (Figs. 3b, S2, S3), which remained virtually unaffected by blank subtraction (Fig. 3c). Apart from that step, no carbon number preference is evident. The *n*-alkanes have $\delta^{13}\text{C}$ values ranging from −29.4 to −33.3‰ (mean $-31.4 \pm 1.2\%$; Fig. 3b; Table 1). The hydropyrolysate also contained isomeric mixtures of C_{12–18} monomethylalkanes (Fig. S3) and a variety of aromatic hydrocarbons, including (dimethyl-, methyl-)naphthalene(s), (methyl-)biphenyl(s), (methyl-)acenaphthene(s), dibenzofuran and (methyl-)phenanthrene(s) (Figs. 3b, c, S4–S6). Biologically diagnostic hydrocarbons such as hopanoids or steroids were absent.

HyPy treatment of excessively pre-extracted biomass of the heterocystous cyanobacterium *Anabaena cylindrica* SAG 1403-2 yielded a variety of organic compounds, but also in-

cluded *n*-alkanes with a clear restriction in carbon number to homologues $\leq n\text{-C}_{18}$ (Fig. 3d). In contrast, our experimental synthesis of abiotic *n*-alkanes through Fischer–Tropsch-type reactions under hydrothermal conditions produced a unimodal distribution of homologues ranging from *n*-C₁₂ to *n*-C₄₁ without any carbon number preference (Fig. 3e).

4 Discussion

4.1 Maturity of the Dresser kerogen

The organic record of Archaean rocks is commonly affected by thermal maturation (Brocks et al., 2008; Brocks, 2011; French et al., 2015). The kerogen within the analysed Dresser sample is thermally mature and structurally disordered, as evidenced by relatively wide D and G bands in the Raman spectra (see Fig. 2c for a representative Raman spectrum). This is also supported by the absence of S1 bands at 2450 cm^{-1} , high R1 ratios (0.98–1.05) and low FWHM-D1 values (68.64–76.12), consistent with prehnite–pumpellyite to lower greenschist metamorphism at a temperature of ca. 300 °C (cf. Yui et al., 1996; Delarue et al., 2016). All of these observations are well in line with published Raman spectra of Archaean organic matter from the same region (Ueno et al., 2001; Marshall et al., 2007; Delarue et al., 2016) and the general thermal history of the host rock (regional prehnite–pumpellyite to lower greenschist metamorphism; Hickman, 1975, 1983, 2012; Terabayashi et al., 2003).

Fitting of D5 peaks can be difficult for Raman spectra of highly mature organic matter (Ferralis et al., 2016). Therefore, the H/C ratios calculated herein (0.03–0.14) should be treated with caution. However, the Raman-based H/C ratios and the methylphenanthrene/phenanthrene value ($\text{MP}/\text{P}=0.33$; Table 2) of the Dresser kerogen are in good accordance with data reported from more mature kerogens from the same region (ca. 3.4 Ga Strelley Pool Formation: 0.08–0.14 and 0.24–0.37, respectively; Marshall et al., 2007). The low methylphenanthrene index ($\text{MPI-I}=0.23$) and high phenanthrene/methylphenanthrene index ($\text{P}/\text{MP}=3.01$) result in a computed vitrinite reflectance (R_c (MPI-I)) of 2.87 (Table 2), indicating a thermal maturity far beyond the oil-generative stage (Radke and Welte, 1983; Boreham et al., 1988). However, it has to be considered that the MPI-I is potentially affected by (de-)methylation reac-

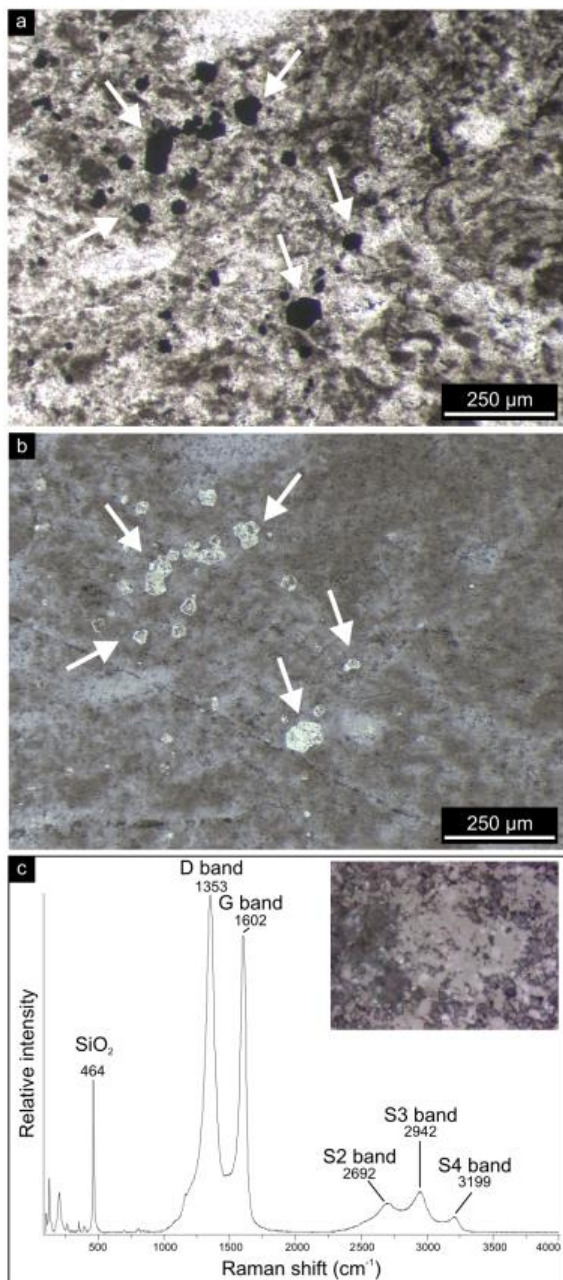


Figure 2. Petrographic observations on the hydrothermal chert vein. (a, b) Thin section photographs (a transmitted light; b reflected light) showing kerogen (brownish colours) and pyrite (arrows, black colours in a, bright colours in b) embedded within a fine-grained chert matrix. Note that the pyrite crystals (arrows) are excellently preserved and show no evidence of oxidation. (c) Representative Raman spectrum of kerogen (D band at 1353 cm^{-1} and G band at 1602 cm^{-1}) present in the hydrothermal chert vein. Note the wide D and G bands (82 and 55 cm^{-1} width, respectively), pointing to thermally mature and structurally disordered kerogen, and the absence of an S1 band (at 2450 cm^{-1}), consistent with prehnite–pumpellyite to lower greenschist metamorphism and a temperature of ca. $300\text{ }^{\circ}\text{C}$ (cf. Yui et al., 1996; Delarue et al., 2016).

tions (Brocks et al., 2003a). The calculated methylnaphthalene ratio (MNR = 2.52; Table 2) corresponds to a somewhat lower mean vitrinite reflectance of ca. 1.5, which is again in line with a post-oil window maturity (cf. Radke et al., 1984). The mismatches between single aromatic maturity parameters are negligible, as these indices have limited application for highly mature Archaean organic matter (Brocks et al., 2003a). The putative offset between the indices and the metamorphic overprint indicated by Raman data is most likely due to the protection of kerogen-bound moieties even under elevated thermal stress (Love et al., 1995; Lockhart et al., 2008). Furthermore, it has been shown that kerogen isolated from the Strelley Pool Formation also contains larger PAH clusters which are not GC-amenable ($> 10\text{--}15$ rings; Marshall et al., 2007). Consequently, it can be anticipated that the compounds detected in the HyPy pyrolysate of the Dresser kerogen represent only a small fraction of the bulk macromolecular organic matter.

The distribution of monomethylalkanes $\leq n\text{-C}_{18}$ (Figs. S3, S4) released from the Dresser kerogen resembles high-temperature HyPy products from the Strelley Pool kerogen (Marshall et al., 2007; their Fig. 15). Such isomeric mixtures are typically formed during thermal cracking of alkyl moieties (Kissin, 1987) and are in good agreement with the estimated maturity range. Methylated aromatics such as methylnaphthalenes and methylphenanthrenes have also been observed in other hydropyrolysates from Archaean kerogens that experienced low-grade metamorphism (Brocks et al., 2003b; Marshall et al., 2007; French et al., 2015). In all of these cases, the degree of alkylation varied with the exact thermal alteration of the respective kerogens (Marshall et al., 2007; French et al., 2015).

4.2 Syngeneity of the Dresser kerogen-derived compounds

The kerogen of the Dresser Formation exclusively occurs in the form of fluffy aggregates and clots embedded within a very dense chert matrix that is, once solidified, highly impermeable to fluids. The depositional age of the formation is constrained to $3481 \pm 3.6\text{ Ma}$ (Van Kranendonk et al., 2008), and the investigated chert vein shows no evidence for disruption by post-depositional hydrothermal fluids. This has also been described for other hydrothermal chert veins of the Dresser Formation, where the kerogen has been interpreted as being syngenetic (i.e. formed prior to host rock lithification; Ueno et al., 2001, 2004; Morag et al., 2016). Furthermore, the maturity of the embedded kerogen is in good accordance with the thermal history of the host rock. An introduction of solid macromolecular organic matter from stratigraphically younger units in this region during later fluid-flow phases, as proposed for the younger Apex chert (Olcott-Marshall et al., 2014), can therefore be excluded.

As the bitumen fractions of Precambrian rocks are easily biased by the incorporation of contaminants during later

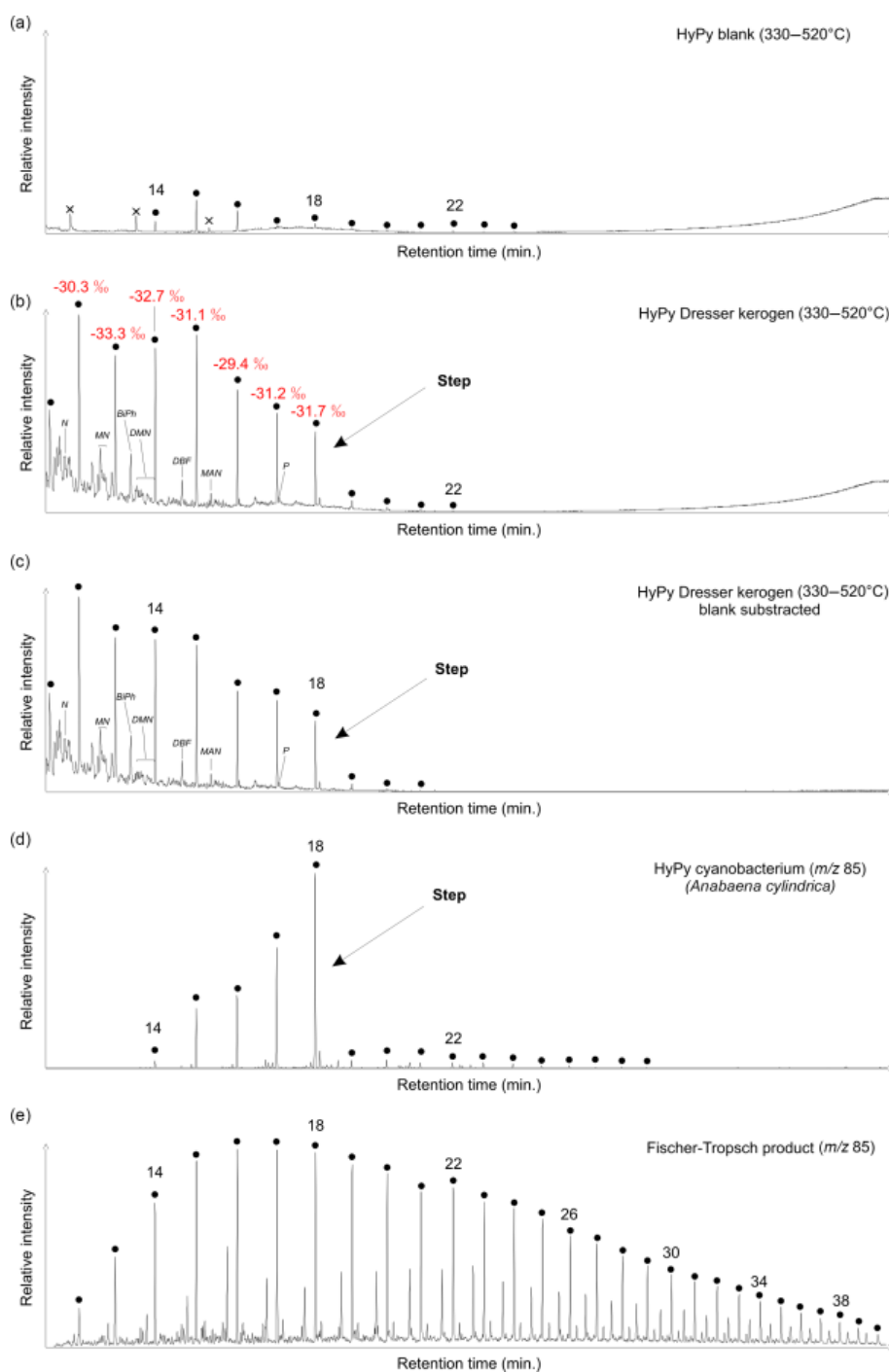


Figure 3. Total ion currents (**a–c**; on the same scale) and ion chromatograms selective for alkanes (**d–e**; m/z 85). **(a)** High-temperature HyPy (330–520 °C) product of analytical blank (combusted sea sand) obtained prior to HyPy of the Dresser kerogen. n -Alkanes in the range of n -C₁₄ to n -C₂₄ (maxima at n -C₁₅) represent HyPy background contamination. **(b)** High-temperature HyPy (330–520 °C) product of the Dresser kerogen. Note the sharp decrease in abundance of n -alkanes beyond n -C₁₈ (see arrows). $\delta^{13}\text{C}$ values of n -C₁₂ to n -C₂₈ show a high similarity to the $\delta^{13}\text{C}_{\text{TOC}}$ value ($-32.8 \pm 0.3\text{‰}$), further confirming syngeneity. **(c)** Blank subtraction (**b** minus **a**) showing that contaminants have no major impact on the n -alkane pattern yielded during the high-temperature HyPy step of the Dresser kerogen (**b**). **(d)** HyPy products of cell material of the heterocystous cyanobacterium *Anabaena cylindrica*. Note the sharp decrease in abundance of n -alkanes beyond n -C₁₈ (see arrows), similar to the n -alkane distribution of the Dresser kerogen (**b**). **(e)** Products of experimental Fischer–Tropsch-type synthesis under hydrothermal conditions; abiogenic n -alkanes show a unimodal distribution that is distinctly different from the Dresser kerogen. Black dots: n -alkanes (numbers refer to carbon chain lengths); N: naphthalene; MN: methylnaphthalenes; BiPh: 1,1'-biphenyl; DMN: dimethylnaphthalenes; DBF: dibenzofuran; MAN: methylacenaphthene; P: phenanthrene; crosses: siloxanes (GC column or septum bleeding).

stages of rock history (Brocks et al., 2008; Brocks, 2011; French et al., 2015), studies have increasingly focussed on kerogen-bound compounds that are more likely to be syngenetic to the host rock (Love et al., 1995; Brocks et al., 2003b; Marshall et al., 2007; French et al., 2015). Potential volatile organic contaminants adhering to the kerogen are removed through excessive extraction and a thermal desorption step ($\sim 350^\circ\text{C}$) prior to high-temperature HyPy (550°C ; cf. Brocks et al., 2003b; Marshall et al., 2007). The recurrence of few *n*-alkanes in the range of *n*-C₁₄ to *n*-C₂₄ (maximum at *n*-C₁₅) in high-temperature HyPy blank runs obtained immediately before and after the actual sample run (Figs. 3a, S2, S3) indicates minor background contamination during pyrolysis, with a source most likely within the HyPy system. However, these contaminants do not significantly affect the *n*-alkane pattern yielded by high-temperature HyPy of the Dresser kerogen, as evidenced by blank subtraction (Fig. 3c).

Contamination of the sample can be further deciphered by the presence of polar additives or hydrocarbons that are not consistent with the thermal history of the host rock. Plastic-derived branched alkanes with quaternary carbon centres (BAQCs), a common contaminant in Precambrian rock samples (Brocks et al., 2008), have not been detected (Fig. S7). Traces of functionalized plasticizers (phenols and phthalic acid; Figs. S2, S6, S8) are unlikely to survive (or result from) HyPy treatment. These compounds are therefore considered as background contamination introduced during sample preparation and analysis after HyPy. The observed siloxanes (Fig. 3, S2) probably originate from the GC column or septum bleeding and are unlikely to be contained in the sample. All of these compounds occur only in low or trace abundances and can be clearly distinguished from the ancient aliphatic and aromatic hydrocarbons contained in the Dresser kerogen.

Contamination by (sub-)recent endoliths can be excluded as sample surfaces have been carefully removed and there is no petrographic indication for borings or fissures containing recent organic material (Fig. 2). HyPy of untreated or extracted biomass would yield a variety of acyclic and cyclic biomarkers (cf. Love et al., 2005). However, high-temperature HyPy of the Dresser kerogen almost exclusively yielded *n*-alkanes, minor amounts of monomethylalkanes and various aromatic hydrocarbons (Figs. 3b, c, S2–S6), while hopanoids or steroids were absent (Figs. S8, S9). This is in good agreement with the maturity of the Dresser kerogen and previous HyPy studies of Archaean rocks (Brocks et al., 2003b; Marshall et al., 2007; French et al., 2015).

Accidental contamination of the kerogen by mono-, di- and triglycerides (e.g. dust, skin surface lipids) can also be ruled out as HyPy treatment of these compounds typically results in *n*-alkane distributions with a distinct predominance of *n*-C₁₆ and *n*-C₁₈ homologues, corresponding to the *n*-C₁₆ and *n*-C₁₈ fatty acid precursors (Craig et al., 2004; Love et al., 2005; unpublished data from our own ob-

servations). At the same time, the observed distribution of kerogen-derived *n*-alkanes, with a distinct decrease beyond *n*-C₁₈ (Fig. 3b, c), is notably similar to high-temperature HyPy products of kerogens isolated from the ca. 3.4 Ga Strelley Pool Formation of the Pilbara Craton (Marshall et al., 2007; their Fig. 14). Marshall and co-workers considered these *n*-alkanes unlikely to be contaminants as they were released only in the high-temperature HyPy step. Furthermore, the stable carbon isotopic composition of *n*-alkanes in the Dresser high-temperature pyrolysate (-29.4 to -33.3‰ ; mean $-31.4 \pm 1.2\text{‰}$) is very similar to the $\delta^{13}\text{C}_{\text{TOC}}$ signature of the sample ($-32.8 \pm 0.3\text{‰}$; Figs. 3, S10; Table 1), indicating that these compounds were generated from the kerogen. Hence, we consider the compounds released from the Dresser kerogen during high-temperature HyPy (Fig. 3b, c) as syngenetic.

High-temperature HyPy of the Dresser kerogen yielded a variety of aromatic hydrocarbons, which are orders of magnitudes lower or absent in all other pyrolysates (Figs. 3, S2, S4–S6). It also produced significantly higher amounts of *n*-alkanes than the low-temperature step, and these further showed a distinct distribution pattern (i.e. a step $\leq n$ -C₁₈; Figs. 3, S2, S3). The lack of even low quantities of *n*-alkenes that typically accompany bond cleavage in kerogen pyrolysis was also observed by Marshall et al. (2007) in their HyPy analysis of cherts from the Strelley Pool Formation. As a possible explanation for the lack of *n*-alkenes, these authors suggested that the *n*-alkanes were not cracked from the kerogen but were rather trapped in closed micropores until the organic host matrix was pyrolytically disrupted. Alternatively, however, unsaturated cleavage products may have been immediately reduced during HyPy by the steadily available hydrogen and catalysts. Indeed, it has been demonstrated that double bonds in linear alkyl chains are efficiently hydrogenated during HyPy, even in the case of pre-extracted microbial biomass (e.g. Love et al., 2005; our Fig. 3d). We consider both as plausible scenarios to explain the absence of *n*-alkenes in the Dresser chert hydropyrolysate.

4.3 Origin of the Dresser kerogen: hydrothermal vs. biological origin

The $\delta^{13}\text{C}_{\text{TOC}}$ value of $-32.8 \pm 0.3\text{‰}$ is consistent with carbon fixation by photo- or chemoautotrophs (cf. Schidlowski, 2001). However, organic compounds exhibiting similar ^{13}C depletions (partly down to ca. -36‰ relative to the initial substrate) could also be formed abiotically during the serpentinization of ultramafic rocks (Fischer–Tropsch-type synthesis; McCollom et al., 1999; McCollom and Seewald, 2006; Proskurowski et al., 2008). A further constraint on the origin of the Dresser kerogen is provided by the distinct decrease in *n*-alkane abundance beyond *n*-C₁₈ observed in the high-temperature HyPy pyrolysate (Fig. 3b, c). This distribution resembles HyPy products of pre-extracted recent cyanobac-

terial biomass, which also shows a very pronounced restriction in carbon number to homologues $\leq n\text{-C}_{18}$ (Fig. 3d).

The pre-extracted cyanobacterial cell material and the abiotically produced *n*-alkanes studied as reference samples experienced no thermal maturation. It can nevertheless be expected that burial, and thus heating, of *Anabaena* biomass (Fig. 3d) would initially liberate lower *n*-alkane homologues from their predominant *n*-alkyl moieties while, up to a certain point, retaining the distinct step at *n*-C₁₈. Experimental maturation of an immature kerogen revealed the preservation of distinct alkyl-chain length preferences even after 100 days at 300 °C (Mißbach et al., 2016; e.g. a step beyond *n*-C₃₁ in their Fig. 2). Further maturation would ultimately lead to a unimodal distribution of short-chain *n*-alkanes and erase the biologically inherited pattern (cf. Mißbach et al., 2016). In contrast, abiotically synthesized extractable organic compounds show a unimodal homologue distribution from the beginning (Fig. 3e) and will retain it, while thermal maturation would gradually shift the *n*-alkane pattern towards shorter homologues. It can therefore be expected that organic compounds cleaved from an abiotic “Fischer–Tropschkerogen” – whose existence has not been proven yet – would also exhibit a unimodal distribution. Consequently, the distinctive distribution of *n*-alkanes released from the Dresser kerogen (i.e. the step $\leq n\text{-C}_{18}$; Figs. 3b, c) can be regarded as a molecular fingerprint relating to a biosynthetic origin of the organic matter.

Highly ¹³C-depleted methane in primary fluid inclusions in hydrothermal chert veins of the Dresser Formation ($\delta^{13}\text{C} < 56\text{‰}$) was taken as evidence for biological methanogenesis and thus the presence of Archaea (Ueno et al., 2006). Our $\delta^{13}\text{C}_{\text{TOC}}$ value ($-32.8 \pm 0.3\text{‰}$; Table 1; Fig. S10) would generally be consistent with both bacterial and archaeal sources (cf. Schidlowski, 2001). Archaea only synthesize isoprene-based compounds (Koga and Morii, 2007; Matsumi et al., 2011). Straight-chain (acetyl-based) hydrocarbon moieties such as fatty acids – the potential precursors of the kerogen-derived *n*-alkanes – are to current knowledge being formed only by Bacteria and Eukarya, where they typically function as constituents of membranes or storage lipids (cf. Erwin, 1973; Kaneda, 1991). The formation of these lipids is tightly controlled by different biosynthetic pathways resulting in characteristic chain-length distributions. In bacterial lipids, carbon chain lengths typically do not extend above *n*-C₁₈ (cf. Kaneda, 1991). Consequently, given the lack of convincing evidence for the presence of Eukarya as early as 3.5 Ga (cf. Parfrey et al., 2011; Knoll, 2014; French et al., 2015), the most plausible source of kerogen-occluded *n*-alkanes in the Dresser hydrothermal chert is Bacteria. Strongly reducing conditions during the deposition of the Dresser Formation are indicated by widespread pyrite, Fe-rich carbonates and trace element signatures (Van Kranendonk et al., 2003, 2008). Potential microbial sources for the Dresser kerogen therefore may have included anoxygenic

photoautotrophic, chemoautotrophic and heterotrophic microorganisms.

4.4 The “hydrothermal pump hypothesis”

Our results strongly support a biological origin of the kerogen found in the early Archaean hydrothermal chert veins of the Dresser Formation. We explain this finding by the redistribution and sequestration of microbial organic matter that may have formed in a variety of Dresser environments through hydrothermal circulation (proposed herein as the “hydrothermal pump hypothesis”; Fig. 4). Higher geothermal gradients prior to the onset of modern-type plate tectonics at ca. 3.2–3.0 Ga (Smithies et al., 2005; Shirey and Richardson, 2011) were possibly important drivers of early Archaean hydrothermal systems. In fact, the Dresser Formation was formed in a volcanic caldera environment affected by strong hydrothermal circulation, where voluminous fluid circulation locally caused intense acid–sulfate alteration of basalts and the formation of a dense hydrothermal vein swarm (Nijman et al., 1999; Van Kranendonk and Pirajno, 2004; Van Kranendonk, 2006; Van Kranendonk et al., 2008; Harris et al., 2009). In addition to the high crustal heat flow, the absence of thick sedimentary cover may have facilitated the intrusion of seawater into the hydrothermal system. The associated large-scale assimilation of particulate and dissolved organic matter and its transport and alteration by hydrothermal fluids (Fig. 4) therefore appears to be a plausible mechanism that may, at least partly, explain the high amounts of kerogen in early Archaean hydrothermal veins.

The hydrothermal pump hypothesis requires a source of organic matter during the deposition of the Dresser Formation (Fig. 4). Whereas contributions from extraterrestrial sources, as well as from Fischer–Tropsch-type synthesis linked to the serpentinization of ultramafic rocks, cannot be excluded, our results indicate a primarily biological origin for the kerogen contained in the chert veins (Fig. 4). The inferred biogenicity is also in line with the consistent $\delta^{13}\text{C}$ offset between bulk kerogens (ca. -20 to -30‰) and carbonate (ca. $\pm 2\text{‰}$) in Archaean rocks (Hayes, 1983; Schidlowski, 2001). Prokaryotic primary producers and heterotrophs may have flourished in microbial mats (Dresser stromatolites; Walter et al., 1980; Van Kranendonk, 2006, 2011; Philippot et al., 2007; Van Kranendonk et al., 2008), the water column (planktic “marine snow”; Brasier et al., 2006; Blake et al., 2010) and even hot springs on land (Djokic et al., 2017). Another biological source for the ancient organic matter could have been chemoautotrophs and heterotrophs thriving in subsurface environments, such as basalts (Banerjee et al., 2007; Furnes et al., 2008) and hydrothermal vent systems (Shen et al., 2001; Ueno et al., 2001, 2004, 2006; Pinti et al., 2009; Morag et al., 2016) (Fig. 4). All of these systems are not mutually exclusive and the largely anoxic conditions would have encouraged a high steady-state abundance of organic matter in the aquatic environment (Fig. 4).

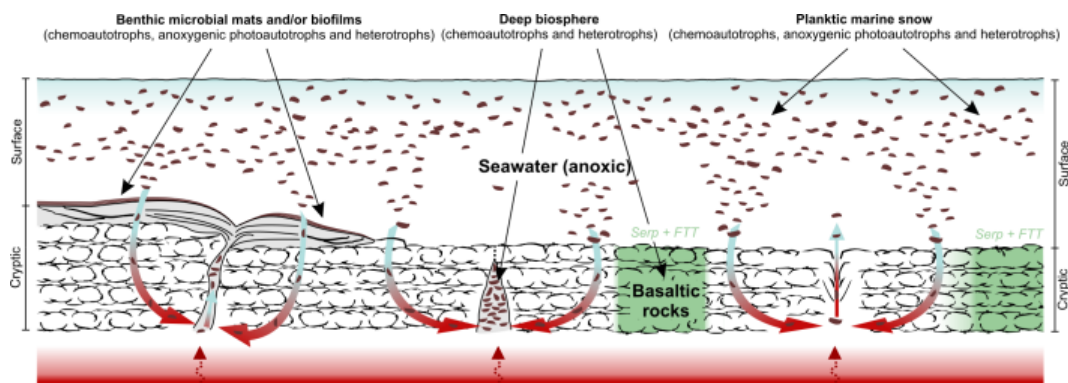


Figure 4. The “hydrothermal pump hypothesis”. Organic matter was predominantly biologically produced and heterotrophically processed by Bacteria and, possibly, Archaea. Additionally, Fischer–Tropsch-type synthesis of organic matter linked to the serpentinization of ultramafic rocks (McCullom et al., 1999; McCullom and Seewald, 2006) may have occurred locally. Primary producers (chemoautotrophs, anoxygenic photoautotrophs) and heterotrophs may have flourished in surface waters (planktic “marine snow”), at the water–rock interface (microbial mats and/or biofilms) and in cryptic environments (e.g. within basalts and hydrothermal vent systems). After accumulating in different Dresser environments, the organic matter was redistributed and sequestered in veins by hydrothermal fluids.

Dissolved organic matter (DOM) in modern seawater may resist decomposition over millennial timescales (Druffel and Griffin, 2015). In recent hydrothermal fields, however, organic matter becomes thermally altered and redistributed (Simoneit, 1993; Delacour et al., 2008; Konn et al., 2009). Laboratory experiments using marine DOM indicate that thermal alteration already occurs at temperatures $> 68\text{--}100\text{ }^{\circ}\text{C}$ and efficient removal of organic molecules at $212\text{--}401\text{ }^{\circ}\text{C}$ (Hawkes et al., 2015, 2016). It has been argued, however, that such DOM removal may also be due to transformation into immiscible material through, for example, condensation (Castello et al., 2014) and/or defunctionalization reactions (Hawkes et al., 2016). These processes, however, are as yet poorly understood. In the Dresser Formation, hydrothermal temperatures ranged from ca. $300\text{ }^{\circ}\text{C}$ at depth to $120\text{ }^{\circ}\text{C}$ near the palaeosurface, causing propylitic (ca. $250\text{--}350\text{ }^{\circ}\text{C}$) and argillic (including advanced argillic: ca. $100\text{--}200\text{ }^{\circ}\text{C}$) alteration of the host rocks (Van Kranendonk and Pirajno, 2004; Van Kranendonk et al., 2008; Harris et al., 2009). Given this variety of thermal regimes, and the generally anoxic nature of early Archaean seawater (e.g. Van Kranendonk et al., 2003, 2008; Li et al., 2013), it is likely that some of the organic substances underwent in situ alteration, but not complete oxidation, during hydrothermal circulation. The entrained organics would have been trapped in the chert that instantaneously precipitated from the ascending hydrothermal fluids due to subsurface cooling (cf. Van Kranendonk, 2006).

In summary, the hydrothermal pump hypothesis proposed here (Fig. 4) includes (i) a net build-up of organic matter in different Dresser environments under largely anoxic conditions, (ii) a large-scale assimilation of particulate and dissolved organic matter from various biological sources and its subsurface transport and alteration by hydrothermal fluids, and (iii) its sequestration within hydrothermal chert veins as

kerogen. This model explains the presence of abundant organic carbon in early Archaean hydrothermal veins, as well as its morphological, structural and isotopic variability observed in the Dresser hydrothermal chert veins (Ueno et al., 2001, 2004; Pinti et al., 2009; Morag et al., 2016). It does not, however, help to pinpoint the formation pathways of distinct carbonaceous structures, as for instance those preserved in the Dresser Formation (Glikson et al., 2008) or the younger Apex chert (e.g. Schopf, 1993; Brasier et al., 2002, 2005; Schopf et al., 2002; Bower et al., 2016). Further work is necessary to test whether consistent molecular and compound-specific isotopic patterns can be generated from a larger set of Archaean kerogens.

5 Conclusions

Kerogen embedded in a hydrothermal chert vein from the ca. 3.5 Ga Dresser Formation (Pilbara Craton, Western Australia) is syngenetic. A biological origin is inferred from the presence of short-chain *n*-alkanes in high-temperature HyPy pyrolysates, showing a sharp decrease in homologue abundance beyond *n*-C₁₈. HyPy products of pre-extracted recent bacterial biomass exhibited a similar restriction to carbon chain lengths $\leq n\text{-C}_{18}$, whereas abiotic compounds experimentally formed via Fischer–Tropsch-type synthesis exhibited a unimodal distribution. A biological interpretation for Dresser organics is further consistent with the $\delta^{13}\text{C}_{\text{TOC}}$ value ($-32.8 \pm 0.3\text{ }^{\circ}\text{‰}$) and the stable carbon isotopic composition of *n*-alkanes in the Dresser high-temperature pyrolysate (-29.4 to $-33.3\text{ }^{\circ}\text{‰}$; mean $-31.4 \pm 1.2\text{ }^{\circ}\text{‰}$). Based on these observations, we propose that the original organic matter was primarily biologically synthesized. We hypothesize that microbially derived organic matter accumulating in anoxic aquatic (surface and/or subsurface) environments was

assimilated, redistributed and sequestered by hydrothermal fluids (“hydrothermal pump hypothesis”).

Data availability. Data are available upon request.

The Supplement related to this article is available online at <https://doi.org/10.5194/bg-15-1535-2018-supplement>.

Author contributions. JPD, JR and MJVK conducted the field work and designed the study. JR conducted petrographic analyses. NS performed Raman spectroscopic analyses. MR and JPD conducted pyrolysis experiments. HM conducted Fischer–Tropsch-type synthesis. TB prepared cyanobacterial cell material. JPD, HM, MR and VT performed biomarker analyses. JPD wrote the manuscript. All authors discussed the results and provided input to the manuscript.

Competing interests. The authors declare that they have no conflict of interest.

Acknowledgements. This work was financially supported by the Deutsche Forschungsgemeinschaft (grant Du 1450/3-1, DFG Priority Programme 1833 “Building a Habitable Earth”, to Jan-Peter Duda and Joachim Reitner; grant Th 713/11-1 to Volker Thiel), the Courant Research Centre of the Georg-August-Universität Göttingen (DFG, German Excellence Program), the Göttingen Academy of Sciences and Humanities (to Jan-Peter Duda and Joachim Reitner), the International Max Planck Research School for Solar System Science at the Georg-August-Universität Göttingen (to Manuel Reinhardt and Helge Mißbach) and the ARC Centre of Excellence for Core to Crust Fluid Systems (Martin J. Van Kranendonk). We thank Martin Blumenberg, Cornelia Conradt, Wolfgang Dröse, Jens Dyckmans, Axel Hackmann, Merve Öztoprak and Burkhard C. Schmidt for scientific and technical support. Josh Rochelmeier is thanked for assistance during sample extraction of *A. cylindrica*. We are indebted to Malcolm Walter and Mark A. van Zuilen for helpful comments on the manuscript and Jack Middelburg for editorial handling. This is publication number 5 of the Early Life Research Group (Department of Geobiology, Georg-August-Universität Göttingen; Göttingen Academy of Sciences and Humanities) and contribution 980 from the ARC Centre of Excellence for Core to Crust Fluid Systems.

We acknowledge support by the German Research Foundation and the Open Access Publication Funds of Georg-August-Universität Göttingen.

This open-access publication was funded by the University of Göttingen.

Edited by: Jack Middelburg

Reviewed by: Mark van Zuilen and Malcolm Walter

References

- Banerjee, N. R., Simonetti, A., Furnes, H., Muehlenbachs, K., Staudigel, H., Heaman, L., and Van Kranendonk, M. J.: Direct dating of Archean microbial ichnofossils, *Geology*, 35, 487–490, <https://doi.org/10.1130/g23534a.1>, 2007.
- Bauersachs, T., Mudimu, O., Schulz, R., and Schwark, L.: Distribution of long chain heterocyst glycolipids in N₂-fixing cyanobacteria of the order Stigonematales, *Phytochemistry*, 98, 145–150, <https://doi.org/10.1016/j.phytochem.2013.11.007>, 2014.
- Blake, R. E., Chang, S. J., and Lepland, A.: Phosphate oxygen isotopic evidence for a temperate and biologically active Archean ocean, *Nature*, 464, 1029–1032, <https://doi.org/10.1038/nature08952>, 2010.
- Boreham, C. J., Crick, I. H., and Powell, T. G.: Alternative calibration of the Methylphenanthrene Index against vitrinite reflectance: Application to maturity measurements on oils and sediments, *Org. Geochem.*, 12, 289–294, [https://doi.org/10.1016/0146-6380\(88\)90266-5](https://doi.org/10.1016/0146-6380(88)90266-5), 1988.
- Bower, D. M., Steele, A., Fries, M. D., Green, O. R., and Lindsay, J. F.: Raman Imaging Spectroscopy of a Putative Microfossil from the ~3.46 Ga Apex Chert: Insights from Quartz Grain Orientation, *Astrobiology*, 16, 169–180, <https://doi.org/10.1089/ast.2014.1207>, 2016.
- Brasier, M. D., Green, O. R., Jephcoat, A. P., Kleppe, A. K., Van Kranendonk, M. J., Lindsay, J. F., Steele, A., and Grassineau, N. V.: Questioning the evidence for Earth’s oldest fossils, *Nature*, 416, 76–81, <https://doi.org/10.1038/416076a>, 2002.
- Brasier, M. D., Green, O. R., Lindsay, J. F., McLoughlin, N., Steele, A., and Stoakes, C.: Critical testing of Earth’s oldest putative fossil assemblage from the ~3.5 Ga Apex chert, Chinaman Creek, Western Australia, *Precambrian Res.*, 140, 55–102, <https://doi.org/10.1016/j.precamres.2005.06.008>, 2005.
- Brasier, M., McLoughlin, N., Green, O., and Wacey, D.: A fresh look at the fossil evidence for early Archean cellular life, *Philos. T. R. Soc. B*, 361, 887–902, <https://doi.org/10.1098/rstb.2006.1835>, 2006.
- Brocks, J. J.: Millimeter-scale concentration gradients of hydrocarbons in Archean shales: Live-oil escape or fingerprint of contamination?, *Geochim. Cosmochim. Ac.*, 75, 3196–3213, <https://doi.org/10.1016/j.gca.2011.03.014>, 2011.
- Brocks, J. J. and Summons, R. E.: Sedimentary Hydrocarbons, Biomarkers for Early Life, in: *Treatise on Geochemistry*, edited by: Holland, H. D. and Turekian, K. K., Pergamon, Amsterdam, the Netherlands, 63–115, 2003.
- Brocks, J. J., Buick, R., Logan, G. A., and Summons, R. E.: Composition and syngeneity of molecular fossils from the 2.78 to 2.45 billion-year-old Mount Bruce Supergroup, Pilbara Craton, Western Australia, *Geochim. Cosmochim. Ac.*, 67, 4289–4319, [https://doi.org/10.1016/S0016-7037\(03\)00208-4](https://doi.org/10.1016/S0016-7037(03)00208-4), 2003a.
- Brocks, J. J., Love, G. D., Snape, C. E., Logan, G. A., Summons, R. E., and Buick, R.: Release of bound aromatic hydrocarbons from late Archean and Mesoproterozoic kerogens via hydropyrolysis, *Geochim. Cosmochim. Ac.*, 67, 1521–1530, [https://doi.org/10.1016/S0016-7037\(02\)01302-9](https://doi.org/10.1016/S0016-7037(02)01302-9), 2003b.
- Brocks, J. J., Grosjean, E., and Logan, G. A.: Assessing biomarker syngeneity using branched alkanes with quaternary carbon (BAQCs) and other plastic contaminants, *Geochim. Cosmochim. Ac.*, 72, 871–888, <https://doi.org/10.1016/j.gca.2007.11.028>, 2008.

- Castello, D., Kruse, A., and Fiori, L.: Supercritical water gasification of hydrochar, *Chem. Eng. Res. Des.*, 92, 1864–1875, <https://doi.org/10.1016/j.cherd.2014.05.024>, 2014.
- Craig, O. E., Love, G. D., Isaksson, S., Taylor, G., and Snape, C. E.: Stable carbon isotopic characterisation of free and bound lipid constituents of archaeological ceramic vessels released by solvent extraction, alkaline hydrolysis and catalytic hydrolysis, *J. Anal. Appl. Pyrol.*, 71, 613–634, <https://doi.org/10.1016/j.jaap.2003.09.001>, 2004.
- Delacour, A., Früh-Green, G. L., Bernasconi, S. M., Schaeffer, P., and Kelley, D. S.: Carbon geochemistry of serpentinites in the Lost City Hydrothermal System (30° N, MAR), *Geochim. Cosmochim. Ac.*, 72, 3681–3702, <https://doi.org/10.1016/j.gca.2008.04.039>, 2008.
- Delarue, F., Rouzaud, J.-N., Derenne, S., Bourbin, M., Westall, F., Kremer, B., Sugitani, K., Deldicque, D., and Robert, F.: The Raman-derived carbonization continuum: A tool to select the best preserved molecular structures in Archean kerogens, *Astrob.*, 16, 407–417, <https://doi.org/10.1089/ast.2015.1392>, 2016.
- Djokic, T., Van Kranendonk, M. J., Campbell, K. A., Walter, M. R., and Ward, C. R.: Earliest signs of life on land preserved in ca. 3.5 Ga hot spring deposits, *Nature Comm.*, 8, 15263, <https://doi.org/10.1038/ncomms15263>, 2017.
- Druffel, E. R. M. and Griffin, S.: Radiocarbon in dissolved organic carbon of the South Pacific Ocean, *Geophys. Res. Lett.*, 42, 4096–4101, <https://doi.org/10.1002/2015gl063764>, 2015.
- Erwin, J. (Ed.): *Lipids and biomembranes of eukaryotic microorganisms*, Acad. Press, New York, USA, 1973.
- Ferralis, N., Matys, E. D., Knoll, A. H., Hallmann, C., and Summons, R. E.: Rapid, direct and non-destructive assessment of fossil organic matter via microRaman spectroscopy, *Carbon*, 108, 440–449, <https://doi.org/10.1016/j.carbon.2016.07.039>, 2016.
- French, K. L., Hallmann, C., Hope, J. M., Schoon, P. L., Zumberge, J. A., Hoshino, Y., Peters, C. A., George, S. C., Love, G. D., Brocks, J. J., and Buick, R.: Reappraisal of hydrocarbon biomarkers in Archean rocks, *P. Natl. Acad. Sci. USA*, 112, 5915–5920, <https://doi.org/10.1073/pnas.1419563112>, 2015.
- Furnes, H., McLoughlin, N., Muehlenbachs, K., Banerjee, N., Staudigel, H., Dilek, Y., de Wit, M., Van Kranendonk, M. J., and Schiffman, P.: Oceanic pillow lavas and hyaloclastites as habitats for microbial life through time – a review, in: *Links Between Geological Processes, Microbial Activities & Evolution of Life*, edited by: Dilek, Y., Furnes, H., and Muehlenbachs, K., Springer, the Netherlands, 1–68, 2008.
- Gérard, E., Moreira, D., Philippot, P., Van Kranendonk, M., and López-García, P.: Modern subsurface bacteria in pristine 2.7 Ga-old fossil stromatolite drillcore samples from the Fortescue Group, Western Australia, *PLoS ONE*, 4, e5298, <https://doi.org/10.1371/journal.pone.0005298>, 2009.
- Glikson, M., Duck, L. J., Golding, S. D., Hofmann, A., Bolhar, R., Webb, R., Baiano, C. F., and Sly, L. I.: Microbial remains in some earliest Earth rocks: Comparison with a potential modern analogue, *Precambrian Res.*, 164, 187–200, <https://doi.org/10.1016/j.precamres.2008.05.002>, 2008.
- Harris, A. C., White, N. C., McPhie, J., Bull, S. W., Line, M. A., Skrzeczynski, R., Mernagh, T. P., and Tosdal, R. M.: Early Archean Hot Springs above Epithermal Veins, North Pole, Western Australia: New Insights from Fluid Inclusion Microanalysis, *Econ. Geol.*, 104, 793–814, <https://doi.org/10.2113/gsecongeo.104.6.793>, 2009.
- Hawkes, J. A., Rossel, P. E., Stubbins, A., Butterfield, D., Connelly, D. P., Achterberg, E. P., Koschinsky, A., Chavagnac, V., Hansen, C. T., Bach, W., and Dittmar, T.: Efficient removal of recalcitrant deep-ocean dissolved organic matter during hydrothermal circulation, *Nat. Geosci.*, 8, 856–860, <https://doi.org/10.1038/ngeo2543>, 2015.
- Hawkes, J. A., Hansen, C. T., Goldhammer, T., Bach, W., and Dittmar, T.: Molecular alteration of marine dissolved organic matter under experimental hydrothermal conditions, *Geochim. Cosmochim. Ac.*, 175, 68–85, <https://doi.org/10.1016/j.gca.2015.11.025>, 2016.
- Hayes, J. M.: Geochemical evidence bearing on the origin of aerobiosis, a speculative hypothesis, in: *The Earth’s Earliest Biosphere: Its Origin and Evolution*, edited by: Schopf, J. W., Princeton University Press, New York, 291–301, 1983.
- Hickman, A. H.: The North Pole barite deposits, Pilbara Goldfield, *Geol. Surv. West. Aust. Ann. Rep.*, 1972, 57–60, 1973.
- Hickman, A. H.: Precambrian structural geology of part of the Pilbara region, *Geol. Surv. West. Aust. Ann. Rep.*, 68–73, 1975.
- Hickman, A. H.: Geology of the Pilbara block and its environs, *Geol. Surv. West. Aust. Bull.*, 127, 1983.
- Hickman, A. H.: Review of the Pilbara Craton and Fortescue Basin, Western Australia: crustal evolution providing environments for early life, *Island Arc*, 21, 1–31, 2012.
- Hickman, A. H. and Van Kranendonk, M. J.: A Billion Years of Earth History: A Geological Transect Through the Pilbara Craton and the Mount Bruce Supergroup – a field guide to accompany 34th IGC Excursion WA-2, *Geol. Surv. West. Aust., Record* 2012/10, 2012.
- Hofmann, A.: Archean Hydrothermal Systems in the Barberton Greenstone Belt and Their Significance as a Habitat for Early Life, in: *Earliest Life on Earth: Habitats, Environments and Methods of Detection*, edited by: Golding, S. and Glikson, M., Springer, Dordrecht, 51–78, https://doi.org/10.1007/978-90-481-8794-2_3, 2011.
- Kaneda, T.: Iso- and Anteiso-Fatty Acids in Bacteria: Biosynthesis, Function, and Taxonomic significance, *Microbiol. Rev.*, 55, 288–302, 1991.
- Killops, S. D. and Killops, V. J.: *Introduction to organic geochemistry*, Blackwell Publ., Malden, USA, 2005.
- Kissin, Y. V.: Catagenesis and composition of petroleum: origin of *n*-alkanes and isoalkanes in petroleum crudes, *Geochim. Cosmochim. Ac.*, 51, 2445–2457, [https://doi.org/10.1016/0016-7037\(87\)90296-1](https://doi.org/10.1016/0016-7037(87)90296-1), 1987.
- Knoll, A. H.: Paleobiological perspectives on early eukaryotic evolution, *CSH Perspect. Biol.*, 6, a016121, <https://doi.org/10.1101/cshperspect.a016121>, 2014.
- Koga, Y. and Morii, H.: Biosynthesis of Ether-Type Polar Lipids in Archaea and Evolutionary Considerations, *Microbiol. Mol. Biol. R.*, 71, 97–120, <https://doi.org/10.1128/mmbr.00033-06>, 2007.
- Konn, C., Charlou, J. L., Donval, J. P., Holm, N. G., Dehairs, F., and Bouillon, S.: Hydrocarbons and oxidized organic compounds in hydrothermal fluids from Rainbow and Lost City ultramafic-hosted vents, *Chem. Geol.*, 258, 299–314, <https://doi.org/10.1016/j.chemgeo.2008.10.034>, 2009.
- Li, W., Czaja, A. D., Van Kranendonk, M. J., Beard, B. L., Roden, E. E., and Johnson, C. M.: An anoxic, Fe(II)-rich, U-poor ocean

- 3.46 billion years ago, *Geochim. Cosmochim. Ac.*, 120, 65–79, <https://doi.org/10.1016/j.gca.2013.06.033>, 2013.
- Lindsay, J. F., Brasier, M. D., McLoughlin, N., Green, O. R., Fogel, M., Steele, A., and Mertzman, S. A.: The problem of deep carbon—An Archean paradox, *Precambrian Res.*, 143, 1–22, <https://doi.org/10.1016/j.precamres.2005.09.003>, 2005.
- Lockhart, R. S., Meredith, W., Love, G. D., and Snape, C. E.: Release of bound aliphatic biomarkers via hydroxyprolysis from Type II kerogen at high maturity, *Org. Geochem.*, 39, 1119–1124, <https://doi.org/10.1016/j.orggeochem.2008.03.016>, 2008.
- Love, G. D., Snape, C. E., Carr, A. D., and Houghton, R. C.: Release of covalently-bound alkane biomarkers in high yields from kerogen via catalytic hydroxyprolysis, *Org. Geochem.*, 23, 981–986, [https://doi.org/10.1016/0146-6380\(95\)00075-5](https://doi.org/10.1016/0146-6380(95)00075-5), 1995.
- Love, G. D., Bowden, S. A., Jahnke, L. L., Snape, C. E., Campbell, C. N., Day, J. G., and Summons, R. E.: A catalytic hydroxyprolysis method for the rapid screening of microbial cultures for lipid biomarkers, *Org. Geochem.*, 36, 63–82, <https://doi.org/10.1016/j.orggeochem.2004.07.010>, 2005.
- Marshall, C. P., Love, G. D., Snape, C. E., Hill, A. C., Allwood, A. C., Walter, M. R., Van Kranendonk, M. J., Bowden, S. A., Sylva, S. P., and Summons, R. E.: Structural characterization of kerogen in 3.4 Ga Archean cherts from the Pilbara Craton, Western Australia, *Precambrian Res.*, 155, 1–23, <https://doi.org/10.1016/j.precamres.2006.12.014>, 2007, 2007.
- Matsumi, R., Atomi, H., Driessen, A. J. M., and van der Oost, J.: Isoprenoid biosynthesis in Archaea – Biochemical and evolutionary implications, *Res., Microbiol.*, 162, 39–52, <https://doi.org/10.1016/j.resmic.2010.10.003>, 2011.
- McCullom, T. M. and Seewald, J. S.: Carbon isotope composition of organic compounds produced by abiotic synthesis under hydrothermal conditions, *Earth Planet. Sc. Lett.*, 243, 74–84, <https://doi.org/10.1016/j.epsl.2006.01.027>, 2006.
- McCullom, T. M., Ritter, G., and Simoneit, B. R. T.: Lipid Synthesis Under Hydrothermal Conditions by Fischer-Tropsch-Type Reactions, *Origins Life Evol. B.*, 29, 153–166, <https://doi.org/10.1023/a:1006592502746>, 1999.
- Meredith, W., Russell, C. A., Cooper, M., Snape, C. E., Love, G. D., Fabbri, D., and Vane, C. H.: Trapping hydroxyprolylates on silica and their subsequent thermal desorption to facilitate rapid fingerprinting by GC-MS, *Organic Geochem.*, 35, 73–89, <https://doi.org/10.1016/j.orggeochem.2003.07.002>, 2004.
- Mißbach, H., Duda, J.-P., Lünsdorf, N. K., Schmidt, B. C., and Thiel, V.: Testing the preservation of biomarkers during experimental maturation of an immature kerogen, *Int. J. Astrobiol.*, 15, 165–175, <https://doi.org/10.1017/S1473550416000069>, 2016.
- Morag, N., Williford, K. H., Kitajima, K., Philippot, P., Van Kranendonk, M. J., Lepot, K., Thomazo, C., and Valley, J. W.: Microstructure-specific carbon isotopic signatures of organic matter from ~3.5 Ga cherts of the Pilbara Craton support a biologic origin, *Precambrian Res.*, 275, 429–449, <https://doi.org/10.1016/j.precamres.2016.01.014>, 2016.
- Nijman, W., de Bruijne, K. H., and Valkering, M. E.: Growth fault control of Early Archean cherts, barite mounds and chert-barite veins, North Pole Dome, Eastern Pilbara, Western Australia, *Precambrian Res.*, 98, 247–274, [https://doi.org/10.1016/S0301-9268\(97\)00062-4](https://doi.org/10.1016/S0301-9268(97)00062-4), 1999.
- Olcott-Marshall, A., Jehlička, J., Rouzaud, J. N., and Marshall, C. P.: Multiple generations of carbonaceous material deposited in Apex chert by basin-scale pervasive hydrothermal fluid flow, *Gondwana Res.*, 25, 284–289, <https://doi.org/10.1016/j.gr.2013.04.006>, 2014.
- Parfrey, L. W., Lahr, D. J., Knoll, A. H., and Katz, L. A.: Estimating the timing of early eukaryotic diversification with multigene molecular clocks, *P. Natl. Acad. Sci. USA*, 108, 13624–13629, <https://doi.org/10.1073/pnas.1110633108>, 2011.
- Peters, K. E., Walters, C. C., and Moldowan, J. M.: *The Biomarker Guide: Volume 2, Biomarkers and Isotopes in Petroleum Exploration and Earth History*, Cambridge University Press, Cambridge, UK, 2005.
- Philippot, P., Van Zuilen, M., Lepot, K., Thomazo, C., Farquhar, J., and Van Kranendonk, M. J.: Early Archean microorganisms preferred elemental sulfur, not sulfate, *Science*, 317, 1534–1537, 2007.
- Pinti, D. L., Hashizume, K., Sugihara, A., Massault, M., and Philippot, P.: Isotopic fractionation of nitrogen and carbon in Paleoproterozoic cherts from Pilbara craton, Western Australia: Origin of ¹⁵N-depleted nitrogen, *Geochim. Cosmochim. Ac.*, 73, 3819–3848, <https://doi.org/10.1016/j.gca.2009.03.014>, 2009.
- Proskurowski, G., Lilley, M. D., Seewald, J. S., Früh-Green, G. L., Olson, E. J., Lupton, J. E., Sylva, S. P., and Kelley, D. S.: Abiogenic hydrocarbon production at Lost City hydrothermal field, *Science*, 319, 604–607, 2008.
- Radke, M. and Welte, D. H.: The Methylphenanthrene Index (MPI): A Maturity Parameter based on Aromatic Hydrocarbons, in: *Advances in Organic Geochemistry 1981: 10th International Meeting on Organic Geochemistry*, Bergen, September 1981, Proceedings, edited by: Bjørøy, M. and European Association of Organic Geochemists, 504–512, Wiley Chichester, 1983.
- Radke, M., Leythaeuser, D., and Teichmüller, M.: Relationship between rank and composition of aromatic hydrocarbons for coals of different origins, *Org. Geochem.*, 6, 423–430, [https://doi.org/10.1016/0146-6380\(84\)90065-2](https://doi.org/10.1016/0146-6380(84)90065-2), 1984.
- Rippka, R., Deruelles, J., Waterbury, J. B., Herdman, M., and Stanier, R. Y.: Generic assignments, strain histories and properties of pure cultures of cyanobacteria, *J. Gen. Microbiol.*, 111, 1–61, <https://doi.org/10.1099/00221287-111-1-1>, 1979.
- Schidlowski, M.: Carbon isotopes as biogeochemical recorders of life over 3.8 Ga of Earth history: evolution of a concept, *Precambrian Res.*, 106, 117–134, [https://doi.org/10.1016/S0301-9268\(00\)00128-5](https://doi.org/10.1016/S0301-9268(00)00128-5), 2001.
- Schopf, J. W.: Microfossils of the Early Archean Apex chert: new evidence of the antiquity of life, *Science*, 260, 640–646, <https://doi.org/10.1126/science.260.5108.640>, 1993.
- Schopf, J. W., Kudryavtsev, A. B., Agresti, D. G., Wdowiak, T. J., and Czaja, A. D.: Laser-Raman imagery of Earth’s earliest fossils, *Nature*, 416, 73–76, <https://doi.org/10.1038/416073a>, 2002.
- Shen, Y., Buick, R., and Canfield, D. E.: Isotopic evidence for microbial sulphate reduction in the early Archean era, *Nature*, 410, 77–81, <https://doi.org/10.1038/35065071>, 2001.
- Shirey, S. B. and Richardson, S. H.: Start of the Wilson Cycle at 3 Ga Shown by Diamonds from Subcontinental Mantle, *Science*, 333, 434–436, <https://doi.org/10.1126/science.1206275>, 2011.
- Simoneit, B. R. T.: Aqueous high-temperature and high-pressure organic geochemistry of hydrothermal vent systems, *Geochim. Cosmochim. Ac.*, 57, 3231–3243, [https://doi.org/10.1016/0016-7037\(93\)90536-6](https://doi.org/10.1016/0016-7037(93)90536-6), 1993.

- Smithies, R. H., Champion, D. C., Van Kranendonk, M. J., Howard, H. M., and Hickman, A. H.: Modern-style subduction processes in the Mesoarchaeon: Geochemical evidence from the 3.12 Ga Whundo intra-oceanic arc, *Earth Planet. Sc. Lett.*, 231, 221–237, <https://doi.org/10.1016/j.epsl.2004.12.026>, 2005.
- Snape, C. E., Bolton, C., Dosch, R. G., and Stephens, H. P.: High liquid yields from bituminous coal via hydrolysis with dispersed catalysts, *Ener. Fuel.*, 3, 421–425, <https://doi.org/10.1021/ef00015a028>, 1989.
- Summons, R. E. and Hallmann, C.: Organic geochemical signatures of early life on earth, in: *Treatise on geochemistry 2nd Ed.*, edited by: Falkowski, P. and Freeman, K., Elsevier, the Netherlands, 33–46, <https://doi.org/10.1016/B978-0-08-095975-7.01005-6>, 2014.
- Terabayashi, M., Masada, Y., and Ozawa, H.: Archean ocean-floor metamorphism in the North Pole area, Pilbara Craton, Western Australia, *Precambrian Res.*, 127, 167–180, [https://doi.org/10.1016/S0301-9268\(03\)00186-4](https://doi.org/10.1016/S0301-9268(03)00186-4), 2003.
- Ueno, Y., Isozaki, Y., Yurimoto, H., and Maruyama, S.: Carbon Isotopic Signatures of Individual Archean Microfossils(?) from Western Australia, *Int. Geol. Rev.*, 43, 196–212, <https://doi.org/10.1080/00206810109465008>, 2001.
- Ueno, Y., Yoshioka, H., Maruyama, S., and Isozaki, Y.: Carbon isotopes and petrography of kerogens in ~3.5-Ga hydrothermal silica dikes in the North Pole area, Western Australia, *Geochim. Cosmochim. Ac.*, 68, 573–589, [https://doi.org/10.1016/S0016-7037\(03\)00462-9](https://doi.org/10.1016/S0016-7037(03)00462-9), 2004.
- Ueno, Y., Yamada, K., Yoshida, N., Maruyama, S., and Isozaki, Y.: Evidence from fluid inclusions for microbial methanogenesis in the early Archean era, *Nature*, 440, 516–519, <https://doi.org/10.1038/nature04584>, 2006.
- Van Kranendonk, M. J.: North Shaw, W.A. Sheet 2755: West. Aust. Geol. Surv. 1 : 100 000, Geol. Series, 1999.
- Van Kranendonk, M. J.: Volcanic degassing, hydrothermal circulation and the flourishing of early life on Earth: A review of the evidence from c. 3490–3240 Ma rocks of the Pilbara Supergroup, Pilbara Craton, Western Australia, *Earth-Sci. Rev.*, 74, 197–240, <https://doi.org/10.1016/j.earscirev.2005.09.005>, 2006.
- Van Kranendonk, M. J.: Morphology as an Indicator of Biogenicity for 3.5–3.2 Ga Fossil Stromatolites from the Pilbara Craton, Western Australia, in: *Advances in Stromatolite Geobiology*, edited by: Reitner, J., Quéric, N.-V., and Arp, G., 537–554, Springer Berlin Heidelberg, 2011.
- Van Kranendonk, M. J. and Pirajno, F.: Geochemistry of metabasalts and hydrothermal alteration zones associated with c. 3.45 Ga chert and barite deposits: implications for the geological setting of the Warrawoona Group, Pilbara Craton, Australia, *Geochem.-Explor. Env. A.*, 4, 253–278, <https://doi.org/10.1144/1467-7873/04-205>, 2004.
- Van Kranendonk, M. J., Webb, G. E., and Kamber, B. S.: Geological and trace element evidence for a marine sedimentary environment of deposition and biogenicity of 3.45 Ga stromatolitic carbonates in the Pilbara Craton, and support for a reducing Archean ocean, *Geobiology*, 1, 91–108, <https://doi.org/10.1046/j.1472-4669.2003.00014.x>, 2003.
- Van Kranendonk, M. J., Philippot, P., Lepot, K., Bodorkos, S., and Pirajno, F.: Geological setting of Earth’s oldest fossils in the ca. 3.5 Ga Dresser Formation, Pilbara Craton, Western Australia. *Precambrian Res.*, 167, 93–124, <https://doi.org/10.1016/j.precamres.2008.07.003>, 2008.
- Walter, M. R., Buick, R., and Dunlop, J. S. R.: Stromatolites 3,400–3,500 Myr old from the North Pole area, Western Australia, *Nature*, 284, 443–445, 1980.
- Yui, T. F., Huang, E., and Xu, J.: Raman spectrum of carbonaceous material: a possible metamorphic grade indicator for low-grade metamorphic rocks, *J. Metamorph. Geol.*, 14, 115–124, <https://doi.org/10.1046/j.1525-1314.1996.05792.x>, 1996.